Magnetic drift kinetic damping of the resistive wall mode in large aspect ratio tokamaks

Yueqiang Liu,[1] M. S. Chu,[2] C. G. Gimblett,[1] and R. J. Hastie[1]
[1]*Euratom/UKAEA Fusion Association, Culham Science Centre, Abingdon, OX14 3DB, United Kingdom*
[2]*General Atomics, San Diego, California 29186, USA*

(Received 18 June 2008; accepted 5 August 2008; published online 16 September 2008)

An analytical, large aspect ratio, calculation of the drift-kinetic energy perturbation is carried out for the resistive wall mode, due to the mode resonance with the magnetic precession drifts of trapped thermal ions and electrons. Four asymptotic cases are identified and analyzed in detail. Generally, a partial stabilization of the mode is possible thanks to the kinetic correction to the perturbed plasma energy. A complete stabilization can occur only in a narrow space of the plasma equilibrium parameters. Kinetic *destabilization* of the mode is also possible due to a finite pressure correction to the precession drift frequency. © *2008 American Institute of Physics*. [DOI: 10.1063/1.2978091]

I. INTRODUCTION

It is well known that advanced tokamaks[1] have good transport properties in the plasma core region, but suffer from a pressure limit set by pressure-driven external kink modes, which are especially vulnerable to instability for a plasma with a broad current profile and a rather peaked pressure profile.[2] A surrounding, highly conducting wall reduces the growth rate of the external kink to a time scale of the vertical field penetration time through the wall, resulting in the so-called resistive wall mode (RWM), which needs to be stabilized for a steady-state operation of advanced scenarios, for example, the Scenario-4 (Ref. 3) designed for the ITER.[4]

Stabilization of the mode by plasma rotation, due to various damping physics, has been a subject of extensive research in recent years, in both theory[5–17] and experiments.[18–28] In particular, recent experiments,[25–28] carried out on the DIII-D (Ref. 29) and JT-60U (Ref. 30) tokamaks, show that the RWM is stable at a very slow plasma rotation, or even in the absence of rotation at some radii. These results cannot be explained with ideal MHD theory involving only the Alfvén continuum damping[17] or the sound wave damping.[6,7,13] While some of the experimental observations, where the plasma has a finite negative toroidal rotation at the plasma edge, can be explained by toroidal simulations involving a semikinetic damping model,[10,25,27] using MARS-F,[31] the same model seems to be incapable of predicting other experimental data, where the plasma rotation is slow everywhere across the whole plasma column. A thorough understanding of the recent experimental results, and a confident prediction for the ITER, require a detailed investigation of the RWM damping physics under various plasma conditions.

At extremely slow plasma rotation, the semikinetic damping model[10] will not be adequate since this model is based on an assumption of the mode resonance with the main ions at bouncing/circulating frequencies. A more probable candidate of the damping model should be based on the mode resonance with particle drifts at even lower frequencies, such as, the magnetic precession drift frequencies of trapped particles studied in Refs. 14 and 15. In fact the latter seems to give a qualitatively correct prediction of the recent experimental observations.

In this work, we carry out an analytical calculation of the drift-kinetic energy perturbation, based on the thermal particle resonance at magnetic drift and electron collision frequencies. We do not consider the contribution from fast particles, which have higher precession drift frequency, hence less resonance with low frequency modes such as the RWM at slow plasma rotation. We follow a similar procedure as in Ref. 10, assuming a large aspect ratio plasma with a circular cross section. The final results clarify various physical effects of the damping.

The stability of the RWM is determined by a dispersion relation generalized from[9]

$$(\gamma + in\omega_E)^2 K + \delta W_p + \frac{\delta W_v^b \gamma \tau_w^* + \delta W_v^\infty}{\gamma \tau_w^* + 1} + \delta W_k = 0, \qquad (1)$$

where γ is the growth rate of the mode, n is the toroidal mode number, ω_E is the (uniform) plasma fluid rotation frequency, K is the kinetic integral of the plasma inertia, δW_p is the perturbed fluid potential energy of the plasma, and δW_v^b and δW_v^∞ are the vacuum energy with and without an ideal conducting wall, respectively. τ_w^* characterizes the wall time of a resistive wall, and δW_k represents the additional energy perturbation term according to the kinetic energy principle theory.[32–37] The goal of this work is to compute δW_k analytically.

The dispersion relation (1) does not include any damping terms arising from kinetic layer contributions, such as, the shear Alfvén damping, which is kinetically enhanced, and does contribute to the mode stabilization normally at fast plasma rotation.[17] This term is naturally absent in the cylindrical model considered in this paper, due to the lack of rational surface inside the plasma.

In Sec. II, we discuss the general assumptions and formalisms associated with the drift-kinetic energy calculation. We carry out the detailed integrations in Sec. III. In Sec. IV, we apply the calculated kinetic energy to estimate the RWM

stability for a cylindrical plasma model with a flat equilibrium current density profile. The work is summarized in Sec. V.

II. PERTURBED DRIFT KINETIC ENERGY IN LARGE ASPECT RATIO PLASMAS

Our calculation is based on the perturbed kinetic energy term, derived by solving analytically the drift kinetic equation in a perturbative manner[35–37]

$$\delta W_k = \frac{1}{2}\sum_{e,i}\sum_{l}\int d^3x \int d\Gamma\left(-\frac{\partial f^0}{\partial \mathcal{E}}\right)Q_l|\langle e^{-i(l+\alpha nq)\omega_b t}H_L\rangle|^2, \tag{2}$$

where the integration is taken in both the real space x and the velocity space Γ. The summation is performed over the plasma species (electrons and ions), and over the Fourier harmonic l while decomposing the perturbed particle distribution function along the unperturbed particle bounce orbit. f^0 is the equilibrium particle distribution function, which we assume to be a Maxwellian

$$f^0(\mathcal{E}) = N\left(\frac{M}{2\pi T}\right)^{3/2} e^{-\mathcal{E}/T},$$

with N the density, M the mass, and T the temperature of the particles. The particle energy $\mathcal{E}=\mathcal{E}_k+e\Phi=Mv^2/2+e\Phi$ consists of the kinetic and potential parts (Φ is the equilibrium electrostatic potential). Q_l represents the mode-particle resonance condition

$$Q_l = \frac{n\omega_{*N}+(\mathcal{E}_k/T-3/2)n\omega_{*T}+n\omega_E-\omega}{(l+\alpha nq)\omega_b+n\omega_d-i\nu_{\text{eff}}+n\omega_E-\omega}, \tag{3}$$

where ω_{*N} and ω_{*T} are the diamagnetic drift frequencies due to the density and temperature gradients, respectively. ω_b denotes the bounce frequency of trapped particles ($\alpha=0$) or the transit frequency of passing ones ($\alpha=1$). ω_d is the bounce-orbit-averaged particle precession drift frequency. q is the equilibrium safety factor. ω_E is the $\vec{E}\times\vec{B}$ plasma fluid rotation frequency, and ω the mode frequency in the laboratory frame, with $n\omega_E-\omega$ being the mode frequency in the plasma frame. n is the toroidal mode number of the mode. Note that generally $\omega=i\gamma$ is a complex number, with $\text{Re}(\gamma)>0$ if the RWM is a growing mode. ν_{eff} is the collision frequency associated with a simple model of the collision operator in the drift kinetic equation. H_L is the perturbed particle energy in the Lagrangian frame

$$H_L = Mv_\parallel^2\vec{\kappa}\cdot\vec{\xi}_\perp+\mu(Q_\parallel+\nabla B\cdot\vec{\xi}_\perp),$$

where $v_\parallel$ is the unperturbed parallel velocity of the particle, κ is the magnetic curvature vector, $\vec{\xi}_\perp$ is the perpendicular component of the plasma displacement, with an $\exp(in\phi)$ dependence on the toroidal angle ϕ, $\mu=Mv_\perp^2/2B$ is the magnetic moment, and B is the equilibrium magnetic field amplitude. Note that we neglect the particle energy term associated with the *perturbed* electrostatic potential, though we keep the *equilibrium* electrostatic potential which drives the $\vec{E}\times\vec{B}$ fluid flow.

The averaging operator $\langle\cdot\rangle$ in Eq. (2) refers to the time average over the unperturbed particle bounce orbit, with t being the time moment in this bounce motion. We notice that in Eq. (2), all the frequencies except ω_E and ω, as well as quantities, such as, $\mathcal{E}_k, T, H_L$, are defined for each particle species, respectively. To avoid excessive indices, we do not put an indicator to distinguish them. The same convention is held in all derivations that follow, except in places where confusion can arise without an explicit indication.

For a large aspect ratio plasma with a circular poloidal cross section, consider a toroidal coordinate system (r,θ,ϕ), with r being the minor radius of the torus, θ and ϕ the poloidal and toroidal angle, respectively. The integration in real space is converted to

$$\int d^3x = 2\pi\int Rrdrd\theta, \tag{4}$$

where $R=R_0(1+\epsilon\cos\theta)$ is the major radius of the torus, with $\epsilon=r/R_0$ the inverse aspect ratio. We assume that the plasma minor radius is normalized to 1, so that R_0 represents effectively the aspect ratio of the torus.

The integration over the velocity space is carried out conventionally over the particle kinetic energy and the magnetic moment

$$\int d\Gamma = \frac{2\pi}{M}\sum_\sigma\iint d\mathcal{E}_k d\mu\frac{B}{\sqrt{2M(\mathcal{E}_k-\mu B)}}, \tag{5}$$

where $\sigma=\text{sign}(v_\parallel)$.

The equilibrium magnetic field, in the large aspect ratio approximation, can be written as

$$\vec{B} = \frac{B_0}{1+\epsilon\cos\theta}\hat{\phi}+\frac{\epsilon}{q}\frac{B_0}{1+\epsilon\cos\theta}\hat{\theta}. \tag{6}$$

To the lowest order in ϵ, $B=|\vec{B}|\simeq B_0(1-\epsilon\cos\theta)$. This allows a simplification of the particle energy integration

$$\int d\Gamma = \frac{\sqrt{2}\pi T^{3/2}}{B_0M^{3/2}}\sum_\sigma\iint d\hat{\mathcal{E}}_k d\lambda\frac{\hat{\mathcal{E}}_k^{1/2}B}{\sqrt{1-\lambda+\lambda\epsilon\cos\theta}}, \tag{7}$$

where $\hat{\mathcal{E}}_k\equiv\mathcal{E}_k/T$, and $\lambda\equiv\mu B_0/\mathcal{E}_k$ is defined as the particle pitch angle.

In a cylinder, the perturbed particle Lagrangian is well approximated[10] by

$$H_L \simeq -\frac{\mathcal{E}_k}{R}(2-\lambda)\xi_R, \tag{8}$$

where ξ_R is the plasma displacement along the major radius.

Substituting Eqs. (4), (7), and (8) into Eq. (2), and carrying out the integration over the poloidal angle θ, we arrive at

$$\delta W_k = \pi^{3/2}\sum_{e,i}\sum_l\sum_\sigma\int dr\epsilon PC_l^2\int d\lambda\frac{(2-\lambda)^2}{F}\times\int d\hat{\mathcal{E}}_k\hat{\mathcal{E}}_k^{5/2}e^{-\hat{\mathcal{E}}_k}Q_l, \tag{9}$$

where P is the equilibrium plasma pressure due to each

species, $C_l(r,\lambda) \equiv |\langle e^{-i(l+\alpha nq)\omega_b t}\xi_R\rangle|$. $F(\epsilon,\lambda)$ is a function defined by Eq. (A1). Following Ref. 10, we first neglect the pitch angle dependence of C_l. Inclusion of the pitch dependence in C_l will be discussed in Sec. IV.

In a large aspect ratio approximation, all the drift frequencies can be calculated analytically. A brief derivation is given in the Appendix, and the results are summarized below

$$\omega_b = \frac{v_{\rm th}}{R_0}\frac{\sigma\sigma_1}{q}\hat{\mathcal{E}}_k^{1/2}F, \tag{10}$$

$$\omega_d = \sigma_2\frac{\rho_L}{r}\frac{v_{\rm th}}{R_0}q\hat{\mathcal{E}}_k D, \tag{11}$$

$$\omega_{*N} = \sigma_2\frac{\rho_L}{r}\frac{v_{\rm th}}{R_0}\frac{1}{4\epsilon}\left(\frac{-r}{N}\frac{dN}{dr}\right), \tag{12}$$

$$\omega_{*T} = \sigma_2\frac{\rho_L}{r}\frac{v_{\rm th}}{R_0}\frac{1}{4\epsilon}\left(\frac{-r}{T}\frac{dT}{dr}\right), \tag{13}$$

where $v_{\rm th} \equiv \sqrt{2T/M}$ is the particle thermal velocity, $\rho_L \equiv v_{\rm th}/\omega_c$ is the Larmor radius of the particle gyromotion, with $\omega_c \equiv eB_0/M$. The parameter $\sigma_1 = 1$ for passing particles, and $\sigma_1 = \sigma/2$ for trapped ones. The parameter $\sigma_2 = 1$ for ions and $\sigma_2 = -1$ for electrons. The normalized magnetic drift $D(\epsilon,\lambda,s)$, with s being the magnetic shear, is defined by Eq. (A8). The normalized bounce F and magnetic drift D frequencies are determined by the equilibrium magnetic geometry and the particle pitch angle.

Note that since $v_{\rm th}^e \gg v_{\rm th}^i$, we have $\omega_b^e \gg \max(\omega_b^i, \omega)$. The electron bounce motion is generally not in resonance with the RWM, hence the electron contribution to δW_k can be neglected in this case. However, since both ions and electrons experience precessional or diamagnetic drifts at the same frequency range (the latter is in fact a fluid drift), both species contribute to the perturbed kinetic energy.

Because of the ρ_L/r scaling, the precession or diamagnetic drift frequencies are normally much smaller than the bounce frequency. Hence, in the resonance condition (3), the precession drift can be neglected as soon as $(l+\alpha nq) \neq 0$, and the diamagnetic drift can be neglected if the plasma rotation frequency is much higher than the diamagnetic frequencies. These are the assumptions made in Ref. 10. {Note that according to Eqs. (10) and (11), ω_d can exceed ω_b for particles with very high energy ($\hat{\mathcal{E}}_k \gg 1$). However, the fraction of such particles [the $\exp(-\hat{\mathcal{E}}_k)$ factor in Eq. (9)] is small}.

In the opposite case, when $(l+\alpha nq)=0$, the particle bounce motion does not participate in the resonance. In addition, the effect of the diamagnetic drift is included if its frequency is comparable to or greater than the plasma rotation frequency. The above two are the assumptions made in Ref. 14 as well as in the analytical derivations presented below. The condition $(l+\alpha nq)=0$ is satisfied either for passing particles ($\alpha=1$) at rational surfaces only, or for trapped particles ($\alpha=0$) with the bounce harmonic number $l=0$. Since the former occurs only in certain radially very narrow regions, and is unlikely to give a significant contribution to δW_k, the precession drifts of passing particles will not be considered. We focus on the resonance contributions only from the trapped ions and electrons, for a specific bounce harmonic $l=0$.

The resonance operator is now written as

$$Q = \frac{n\omega_{*N} + (\hat{\mathcal{E}}_k - 3/2)n\omega_{*T} + n\omega_E - \omega}{n\omega_d - i\nu_{\rm eff} + n\omega_E - \omega}, \tag{14}$$

and the kinetic integral is simplified to

$$\delta W_k = 2\pi^{3/2}\sum_{e,i}\int dr\epsilon P C_{l=0}^2 \int d\lambda \frac{(2-\lambda)^2}{F} I(r,\lambda), \tag{15}$$

where a factor of 2 appears after summation Σ_σ, $C_{l=0} = |\langle \xi_R\rangle|$ is the bounce orbit average of the displacement along the major radius, and

$$I \equiv \int d\hat{\mathcal{E}}_k \hat{\mathcal{E}}_k^{5/2} e^{-\hat{\mathcal{E}}_k} Q. \tag{16}$$

In the next section, we first evaluate δW_k, Eq. (15) in various limits, then make a calculation under general conditions.

III. KINETIC ENERGY DUE TO PRECESSION DRIFTS OF TRAPPED PARTICLES

A. Very slow plasma rotation

In this limit, we consider a collisionless plasma with rotation frequency much smaller than the particle precessional frequency, i.e., $\max(\nu_{\rm eff}, |n\omega_E - \omega|) \ll |\omega_d|$. The resonance operator becomes

$$Q^{(a)} = \frac{\hat{\mathcal{E}}_k\omega_{*T} + (\omega_{*N} - 3/2\omega_{*T})}{\hat{\mathcal{E}}_k C_d D}, \tag{17}$$

where $C_d \equiv \sigma_2 q(\rho_L/r)(v_{\rm th}/R_0)$. Note that since both precessional and diamagnetic frequencies depend on the sign of the particle charge, $Q^{(a)}$ has the same sign for both ions and electrons. The integration over the particle energy Eq. (16) is performed by substituting the variable $\hat{\mathcal{E}}_k \to u^2$, and using the identity

$$\int_0^\infty u^{2p}e^{-u^2}du = \frac{\Gamma(p+1/2)}{2}, \quad p = 0,1,2,\ldots.$$

We obtain

$$I^{(a)} = -\frac{3\sqrt{\pi}}{16}\frac{R_0}{qD}\frac{d\ln P}{dr},$$

and

$$\delta W_k^{(a)} = \frac{3\pi^2}{8}\sum_{i,e}\int_0^1 dr C_{l=0}^2 \frac{r}{q}\left(-\frac{dP}{dr}\right)G(r), \tag{18}$$

where the factor G represents the final integral over the particle pitch angle

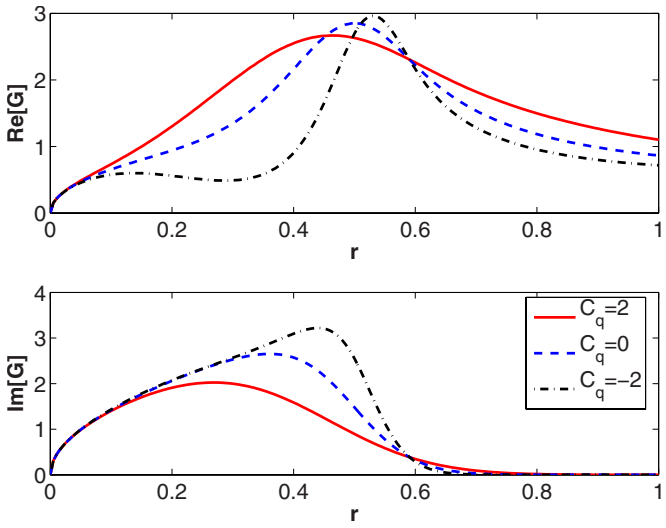

FIG. 1. (Color online) The radial profiles of the normalized integral over the velocity space G, corresponding to the three q profiles of Fig. 2. Only the positive branch of Im(G) is plotted. A major radius $R_0=3$ is assumed.

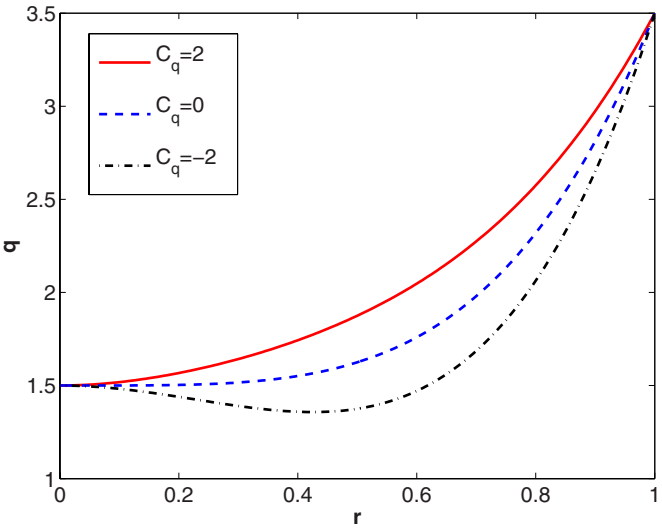

FIG. 2. (Color online) Analytical q profiles $q=1.5+C_q r^2(1-r)+2r^4$, with $C_q=2,0,-2$, respectively.

$$G(r) \equiv \int_{1/(1+\epsilon)}^{1/(1-\epsilon)} d\lambda \frac{(2-\lambda)^2}{FD}. \tag{19}$$

Equation (18) shows that the perturbed kinetic energy is proportional to the equilibrium pressure gradient, as a result of inclusion of the diamagnetic drifts. Note that for a general q-profile, G is a function of the minor radius r rather than the inverse aspect ratio ϵ.

We need to pay special attention to the pitch angle integral Eq. (19). Equation (A8) shows that $D[\lambda_{\min} \equiv 1/(1+\epsilon)] = -0.5/(1+\epsilon) < 0$, and $D[\lambda_{\max} \equiv 1/(1-\epsilon)] = 0.5/(1-\epsilon) > 0$, independent of the choice of the magnetic shear. Hence at all minor radii, there is a pitch angle $\lambda_0 \in (\lambda_{\min}, \lambda_{\max})$, such that $D(\lambda_0)=0$. Near the root λ_0, $D(\lambda)$ is approximated by

$$D(\lambda) = D'(\lambda_0)(\lambda - \lambda_0) + \cdots,$$

where the derivative $D'(\lambda_0)$ generally does not vanish, and rapidly becomes large with increasing magnetic shear. The integration of the $1/x$ type of function in Eq. (19) yields an imaginary part

$$\mathrm{Im}[G] = \frac{(2-\lambda_0)^2}{F(\lambda_0)} \frac{(\pm\pi)}{|D'(\lambda_0)|}, \tag{20}$$

where the $\pm$ sign depends on how we go around the pole in performing the integration. The above approach for computing Im[G] is ambiguous from the physics point of view. A rigorous procedure, given in Sec. III E, will show that this imaginary part comes from the Landau resonance damping, and the sign of Im[G] changes when we switch from ions to electrons. Consequently, the imaginary parts of $\delta W_k^{(a)}$ from ions and electrons cancel each other. A complete cancellation occurs when $T_i=T_e$. The real parts of the contributions from ions and electrons do not cancel according to Eq. (18).

The normalized integral over the velocity space G is affected by the magnetic shear via the D factor, see Eq. (A8). Figure 1 shows the radial profile of the real and imaginary parts of G, respectively, for one particle species and for three types of the equilibrium q profile, defined analytically as

$$q = 1.5 + C_q r^2(1-r) + 2r^4.$$

Three choices of the parameter $C_q=2,0,-2$ give the corresponding q profiles shown in Fig. 2. We notice that the imaginary part of the kinetic energy is as large as the real part, both reaching a maximum around the middle of the plasma minor radius. The shape of the G profile depends sensitively on the magnetic shear. In particular, the q profile with a reversed central shear shrinks both the real and the imaginary parts of the G profile. Close to $r=0$, $G(r) \sim r^{1/2}$ for both the real and imaginary parts.

B. Very fast plasma rotation

In this limit, we assume $|n\omega_E - \omega| \gg \max(|\omega_{*N}|, |\omega_{*T}|, |\omega_d|, \nu_{\mathrm{eff}})$. This can be viewed as the Kruskal–Oberman high-frequency limit[32] for trapped ions and electrons (for bounce harmonic $l=0$ only). It is trivial to show that

$$Q^{(b)} = 1, \quad I^{(b)} = \frac{15}{8}\sqrt{\pi},$$

and

$$\delta W_k^{(b)} = \frac{15\pi^2}{4} \int_0^1 dr C_{l=0}^2 \epsilon P_{\mathrm{eq}} S(r), \tag{21}$$

where $P_{\mathrm{eq}} \equiv P_i + P_e$ is the total equilibrium pressure, and

$$S(\epsilon) \equiv \int_{1/(1+\epsilon)}^{1/(1-\epsilon)} d\lambda \frac{(2-\lambda)^2}{F}. \tag{22}$$

We note that $\delta W_k^{(b)}$ is real, positive, proportional to the total equilibrium pressure P_{eq}, and independent of the safety factor q or the magnetic shear s. The radial dependence of the factor S is plotted in Fig. 3, showing a monotonic increase with ϵ, and $S \sim \epsilon^{1/2}$ at ϵ near 0.

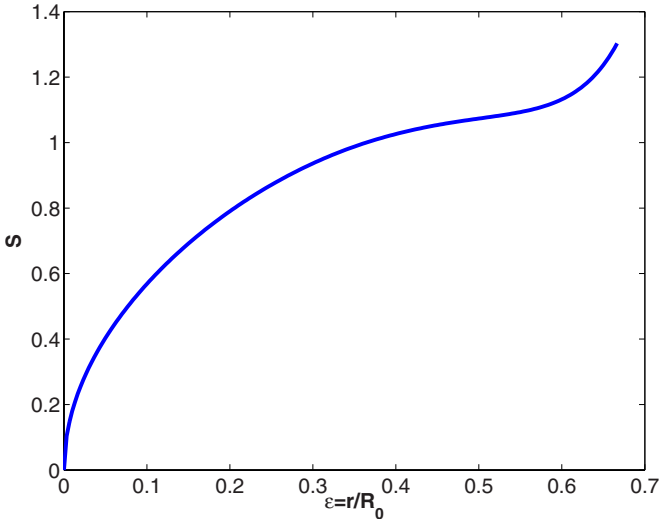

FIG. 3. (Color online) The radial profile of the S factor. A major radius $R_0=3$ is assumed.

C. Slow but finite plasma rotation

In this limit, we assume $\max(|\omega_d|, \nu_{\text{eff}}) \ll |n\omega_E - \omega| \sim (|\omega_{*N}|, |\omega_{*T}|)$. Neglecting the precession drifts in Eq. (14), we obtain

$$Q^{(c)} = 1 + \frac{\hat{\mathcal{E}}_k n\omega_{*T} + n(\omega_{*N} - 3/2\omega_{*T})}{n\omega_E - \omega}, \tag{23}$$

and

$$I^{(c)} = \frac{15\sqrt{\pi}}{8}\left[1 + \frac{n(\omega_{*N} + 2\omega_{*T})}{n\omega_E - \omega}\right]. \tag{24}$$

We further assume that the ions and electrons have the same equilibrium temperature profile, and introduce a fraction parameter C_p such that

$$T_i = C_p T_{\text{eq}} \equiv C_p(T_i + T_e), \quad P_i = C_p P_{\text{eq}}.$$

The identity

$$\sum_{j=e,i} P_j(\omega^j_{*N} + 2\omega^j_{*T}) = (1 - 2C_p)\frac{1}{2re}\frac{d(P_{\text{eq}}T_{\text{eq}})}{dr}$$

helps us to derive the final expression for the perturbed drift kinetic energy

$$\delta W_k^{(c)} = \delta W_k^{(b)} + (1 - 2C_p)\frac{15\pi^2}{8}\frac{1}{eR_0} \times \int_0^1 drC^2_{l=0}\frac{n}{n\omega_E - \omega}\frac{d(P_{\text{eq}}T_{\text{eq}})}{dr}S(r). \tag{25}$$

Note that the second term on the RHS of Eq. (25) vanishes at $C_p=0.5$ (i.e., $T_i=T_e$), due to the exact cancellation of the kinetic contribution between ions and electrons. Otherwise, this term is inversely proportional to $(n\omega_E - \omega)$, and hence tends to be large when the plasma rotation becomes slow (yet still faster than the particle precessional drifts). If the RWM is a growing mode, i.e., $\text{Im}(\omega) > 0$, the second term also provides a pure damping contribution [the imaginary part of $\delta W_k^{(c)}$] to the mode stabilization. Finally, we notice that the second term presents a FLR correction to the first one.

D. Collisional plasma limit

Here we assume $\max(|\omega_d^e|, |n\omega_E - \omega|) \ll \nu^e_{\text{eff}}$, which is most likely valid in the plasma edge region, where both the plasma rotation speed and the temperature are low. Considering only the electron collisions, since the ion collision frequency is much smaller, we have

$$Q^{(d)} = i\frac{\hat{\mathcal{E}}_k n\omega^e_{*T} + n(\omega^e_{*N} - 3/2\omega^e_{*T})}{\nu^e_{\text{eff}}}. \tag{26}$$

Generally, $\nu_{\text{eff}} = \nu/\epsilon$ is a function of the particle energy. Neglecting the energy dependence of ν^e_{eff}, we can make a crude estimation for

$$I^{(d)} \simeq i\frac{15\sqrt{\pi}}{8}\frac{n(\omega^e_{*N} + 2\omega^e_{*T})}{\nu^e_{\text{eff}}}, \tag{27}$$

and for the perturbed kinetic energy

$$\delta W_k^{(d)} \simeq i(1 - C_p)^2\frac{15\pi^2}{8}\frac{1}{eR_0}\int_0^1 drC^2_{l=0}\frac{n}{\nu^e_{\text{eff}}}\frac{d(P_{\text{eq}}T_{\text{eq}})}{dr}S(r), \tag{28}$$

which represents a pure damping on the mode. This kinetic contribution is inversely proportional to the electron collision frequency, which in turn is proportional to $NT_e^{-3/2}$.

E. General case

Without any ordering of the terms, the resonance operator Q of Eq. (14) can be rewritten as

$$Q = \frac{\hat{\mathcal{E}}_k\Omega^b_* + \Omega^a_* + \Omega_n}{\hat{\mathcal{E}}_k + \Omega_n}, \tag{29}$$

where we have introduced

$$\Omega_n = \frac{n\omega_E - \omega - i\nu_{\text{eff}}}{nC_dD}, \quad \Omega^a_* = \frac{n\omega_{*N} - \frac{3}{2}n\omega_{*T} + i\nu_{\text{eff}}}{nC_dD},$$

$$\Omega^b_* = \frac{n\omega_{*T}}{nC_dD}.$$

The energy integral (16) is carried out analytically (again neglecting the particle energy dependence of ν^e_{eff}),

$$I = \frac{15\sqrt{\pi}}{8}\Omega^b_* + 2\sqrt{\pi}(\Omega_n + \Omega^a_* - \Omega_n\Omega^b_*) \times \left[\frac{3}{8} - \frac{1}{4}\Omega_n + \frac{1}{2}\Omega_n^2 + i\frac{1}{2}\Omega_n^{5/2}Z(i\Omega_n^{1/2})\right], \tag{30}$$

where Z is the plasma dispersion function[42]

$$Z(y) = \frac{1}{\sqrt{\pi}} \int_{-\infty}^{\infty} \frac{e^{-u^2}}{u - y} du.$$

In Eq. (30), for an unstable mode $\mathrm{Im}(\omega) > 0$, we always choose the branch of $\Omega_n^{1/2}$ that lies in quadrants I or IV of the complex plane. The perturbed drift kinetic energy δW_k is computed by substituting Eq. (30) into Eq. (15).

In the limit when $\Omega_n = 0$ and $\nu_{\mathrm{eff}} = 0$, we recover the case A

$$I = \frac{15\sqrt{\pi}}{8} \Omega_*^b + \frac{3\sqrt{\pi}}{4} \Omega_*^a \equiv I^{(a)}.$$

Now we derive rigorously the Landau damping term in this limit. For simplicity we shall assume $\nu_{\mathrm{eff}} = 0, \omega_E = 0$ and allow a very small but finite real ω. For definiteness, we assume that $\omega > 0, n = -1$. The resonance condition (29) requires $\Omega_n < 0$, which is satisfied for those ions with pitch angle $\lambda \in (\lambda_{\min}, \lambda_0)$, where λ_0, as before, is the root of $D(\lambda) = 0$. For electrons, the resonance occurs for $\lambda \in (\lambda_0, \lambda_{\max})$. In either case, we introduce a new variable $y = \sqrt{-\Omega_n}$. The Landau resonance in the particle energy space yields an imaginary part for the energy integral factor I following Eq. (16),

$$\mathrm{Im}[I] = -\pi e^{-y^2} \left[\left(1 + \frac{\omega_{*N} - 3/2\omega_{*T}}{\omega} \right) y^7 + \frac{\omega_{*T}}{\omega} y^9 \right],$$

where we have used the fact that

$$\mathrm{Im}[Z(y)] = \sqrt{\pi} e^{-y^2}.$$

Performing the pitch angle integration of $\mathrm{Im}\{I[y(\lambda)]\}$ on $(\lambda_{\min}, \lambda_0)$ for ions, or on $(\lambda_0, \lambda_{\max})$ for electrons, and allowing $\omega \to 0$, we eventually obtain expression (20), where we take the $-$ sign for ions and $+$ sign for electrons.

Case B is recovered by assuming $\Omega_n \to \infty$ and applying the asymptotic expansion of the Z function

$$Z(y) = i\sqrt{\pi} \sigma_3 e^{-y^2} - \frac{1}{\sqrt{\pi}} \sum_{p=0}^{\sim[|y|^2]} \Gamma(p + 1/2) y^{-(2p+1)}, \quad |y| \gg 1,$$

where $\sigma_3 = 1$ if y is real, and $\sigma_3 = 1 - \mathrm{sign}[\mathrm{Im}(y)]$ otherwise.

We can obtain the case C if we set $\nu_{\mathrm{eff}} = 0$ and allow $\Omega_n, \Omega_*^a, \Omega_*^b$ all to approach infinity while keeping their ratio

$$\frac{\Omega_*^a}{\Omega_n} = \frac{n(\omega_{*N} - 3/2\omega_{*T})}{n\omega_E - \omega}, \quad \frac{\Omega_*^b}{\Omega_n} = \frac{n\omega_{*T}}{n\omega_E - \omega}.$$

In this case the lowest order term in the asymptotic expansion of the I factor becomes

$$I = \frac{15}{8}\sqrt{\pi}\left(1 + \frac{\Omega_*^a}{\Omega_n} \right) + \frac{105}{16}\sqrt{\pi}\frac{\Omega_*^b}{\Omega_n} \equiv I^{(c)}.$$

In case C, the second term in Eq. (25) vanishes when $C_p = 0.5$, i.e., when the ion and the electron equilibrium temperatures become equal. Since this is an important case relevant to ITER plasmas, let us consider the next order FLR correction term to $\delta W_k^{(c)}$, using a better asymptotic for the I factor calculated in Eq. (30),

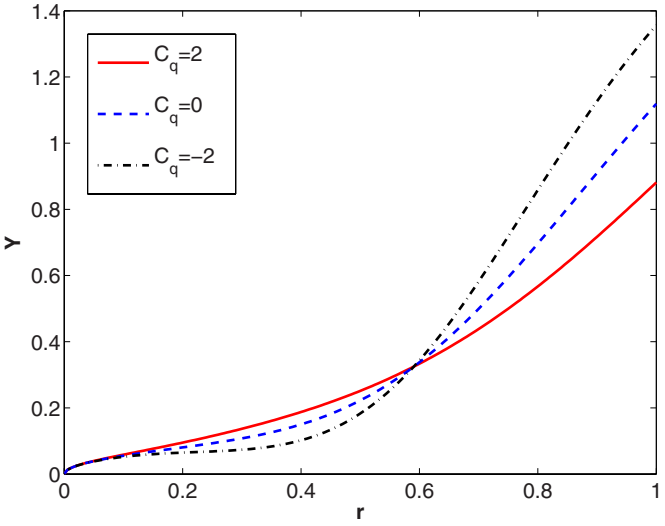

FIG. 4. (Color online) The radial profiles of the Y factor, corresponding to the three q profiles. A major radius $R_0 = 3$ is assumed.

$$\frac{I}{\sqrt{\pi}} = \frac{15}{8} + \frac{15}{8}\frac{\Omega_*^a}{\Omega_n} - \frac{105}{16}\frac{1 - \Omega_*^b}{\Omega_n} - \frac{105}{16}\frac{\Omega_*^a}{\Omega_n^2} + \frac{945}{32}\frac{1 - \Omega_*^b}{\Omega_n^2} + \cdots,$$

$$\min(|\Omega_n|, |\Omega_*^a|, |\Omega_*^b|) \gg 1.$$

Neglecting the plasma collisions, putting together the ion and electron contributions, and after cancellation of the first order terms at $C_p = 0.5$, we arrive at

$$\frac{I_i + I_e}{\sqrt{\pi}} = \frac{15}{4} - \frac{105}{8}\frac{\Omega_{*i}^a}{\Omega_{ni}^2} - \frac{945}{16}\frac{\Omega_{*i}^b}{\Omega_{ni}^2} \tag{31}$$

$$= \frac{15}{4} - \frac{105}{8}\frac{n^2}{(n\omega_E - \omega)^2} C_d^i D(\omega_{*N}^i + 3\omega_{*T}^i). \tag{32}$$

Substitution of Eq. (32) into Eq. (15) gives

$$\delta W_k^{C_p = 0.5} = \delta W_k^{(b)} + \frac{105\pi^2}{32} \frac{1}{e^2 R_0^2 B_0^2} \times \int_0^1 dr C_{l=0}^2 \frac{n^2}{(n\omega_E - \omega)^2} \frac{q}{r} \frac{d(P_{\mathrm{eq}} T_{\mathrm{eq}}^2)}{dr} Y(r), \tag{33}$$

where

$$Y(r) \equiv \int_{1/(1+\epsilon)}^{1/(1-\epsilon)} d\lambda (2 - \lambda)^2 \frac{D}{F}. \tag{34}$$

Note that the second term on the RHS of Eq. (33) is inversely proportional to $(n\omega_E - \omega)^2$. The factor $Y(r)$ is plotted in Fig. 4 for various q profiles. No qualitative change of the Y profile is observed over a rather significant variation of the q profile. This factor generally increases from the plasma center towards the edge.

The trapped particle precession drifts can be strongly affected by the plasma equilibrium pressure gradient,[41]

which in turn modifies the normalized integrals G and Y over velocity space in the kinetic energy terms. According to the large aspect ratio calculation in Ref. 41, the normalized magnetic drift D, defined in Eq. (A8), is corrected by the additional diamagnetic terms

$$D_P = D - \alpha_P \lambda \left\{ \frac{1}{4q^2} + \frac{2}{3}\left[\frac{\hat{E}(k_t)}{\hat{K}(k_t)}(2k_t^2 - 1) + (1 - k_t^2) \right] \right\}, \tag{35}$$

where $\alpha_P = -(2\mu_0 R_0/B_0^2)q^2(dP_{\mathrm{eq}}/dr)$. The consequence of these new terms on the kinetic modification of the RWM stability is clarified in the next section.

IV. APPLICATION TO A CYLINDRICAL PLASMA

A. Brief description of the fluid model

We consider a cylindrical plasma equilibrium with circular cross section and a flat current density $\vec{J} = J_0\hat{z}$.[43] In the cylindrical coordinate system (r, θ, z), the equilibrium magnetic field is

$$\vec{B} = B_0\hat{z} + B_\theta\hat{\theta},$$

where $B_\theta = \mu_0 J_0 r/2$ inside the plasma, $0 \leqslant r \leqslant 1$. The q profile is also flat, with $q(r) = q_0 \equiv 2B_0/(\mu_0 R_0 J_0)$, and R_0 effectively defines the aspect ratio in a toroidal geometry. The equilibrium force balance condition determines a parabolic pressure profile

$$P_{\mathrm{eq}}(r) = P_0(1 - r^2),$$

with $P_0 = \mu_0 J_0^2/4$. The normalized plasma pressure $\beta_N \equiv \beta[\%]/(I[\mathrm{MA}]/a[\mathrm{m}]B_0[\mathrm{T}]) = 20/(q_0 R_0)$, with $\beta = <P_{\mathrm{eq}}>_v/(B_0^2/2\mu_0)$, and $\langle\cdot\rangle_v$ denoting the average over the plasma volume.

Assuming further a flat plasma density $\rho(r) = \rho_0$, it is well known that the current-driven ideal kink of form $\exp(im\theta + inz/R_0)$ has a growth rate[44]

$$(\gamma\tau_A)^2 = \frac{2q_0^2}{(m + nq_0)^2}\left[\frac{\nu}{m + nq_0} - \frac{1}{1 - b^{-2\mu}} \right], \tag{36}$$

where $\tau_A = \omega_A^{-1} \equiv \sqrt{\mu_0\rho_0}R_0/B_0$, $\mu \equiv |m|$, $\nu = m/\mu$, and (m,n) are the poloidal and toroidal mode numbers, respectively. b is the radial position of an ideal conducting wall, normalized by the plasma minor radius.

In the presence of a resistive wall at the radial position b, the ideal kink becomes a RWM, with the growth rate (neglecting the plasma inertia)

$$\gamma\tau_w = -\mu\frac{1 - \nu(m + nq_0)}{1 - \nu(m + nq_0) - b^{-2\mu}}, \tag{37}$$

where τ_w is defined as the field penetration time for the $m=1$ wall mode: $\tau_w = \mu_0\sigma r_w d/2$, with σ the wall conductivity and d the wall thickness.

We wish to estimate the drift kinetic modification of the RWM stability using the dispersion relation (1), which, after neglecting the plasma inertia term, can be rewritten as

$$\gamma\tau_w^* = -\frac{\delta W_f^\infty + \delta W_k}{\delta W_f^b + \delta W_k}, \tag{38}$$

where $\delta W_f^\infty \equiv \delta W_p + \delta W_v^\infty$, $\delta W_f^b \equiv \delta W_p + \delta W_v^b$ are the perturbed fluid energy of the ideal kink mode with and without an ideal wall, respectively. Knowing the growth rate of the ideal kink Eq. (36), the fluid potential energies are easily calculated via the energy principle for ideal kink modes

$$\gamma^2\delta K + \delta W_f = 0, \tag{39}$$

where δK is the kinetic energy associated with the plasma inertia

$$\delta K = \frac{1}{2}\int dx^3 \rho |\vec{\xi}_\perp|^2. \tag{40}$$

For an equilibrium with flat current and density profiles, the eigenfunction for the plasma displacement $\vec{\xi}$ is expressed by

$$\vec{\xi} = \nabla_\perp \zeta \times \hat{z}, \tag{41}$$

where $\zeta = -i\psi/F_0$, and $\psi(r) = r^\mu$ is the eigenfunction for the perturbed magnetic flux inside the plasma, $F_0 \equiv (m + nq_0)B_\theta/r = B_0(m + nq_0)/(R_0 q_0)$. Substitution of Eq. (41) into Eq. (40) yields

$$\delta K = 2\pi^2 R_0 \tau_A^2 \frac{\mu}{\mu_0}\frac{q_0^2}{(m + nq_0)^2}, \tag{42}$$

in which we have neglected terms associated with higher order large aspect ratio expansion. Note that the cylindrical $(\gamma\tau_A)^2$ scaling of the inertial energy is due to the absence of rational surfaces. In a toroidal plasma, internal resonance layers will most likely give a dominant contribution to an ideal mode, that scales as $(\gamma\tau_A)$. However, for the RWM, where the plasma inertia normally plays a minor role, δK does not enter into the final dispersion relation (38). The only purpose that we compute δK here is to evaluate the potential energy, which is finally obtained by combining Eqs. (36), (39), and (42),

$$\delta W_f^\infty = -4\pi^2 R_0 \frac{\mu}{\mu_0}\left(\frac{\nu}{m + nq_0} - 1 \right), \tag{43}$$

$$\delta W_f^b = -4\pi^2 R_0 \frac{\mu}{\mu_0}\left(\frac{\nu}{m + nq_0} - \frac{1}{1 - b^{-2\mu}} \right). \tag{44}$$

In the absence of the drift kinetic effects, it is easy to verify that

$$\gamma\tau_w^* = -\frac{\delta W_f^\infty}{\delta W_f^b} = -\frac{1 - \nu(m + nq_0)}{1 - \nu(m + nq_0) - b^{-2\mu}}(1 - b^{-2\mu}) = \gamma\tau_w(1 - b^{-2\mu})/\mu, \tag{45}$$

where we identify $\tau_w^* = \tau_w(1 - b^{-2\mu})/\mu$.

B. Drift kinetic modification of the RWM stability

In the presence of the drift kinetic effect, the growth rate of the mode is modified according to Eq. (38), in which we shall use the δW_k calculated in the previous section. Note that we are combining δW_k calculated for a large aspect ratio

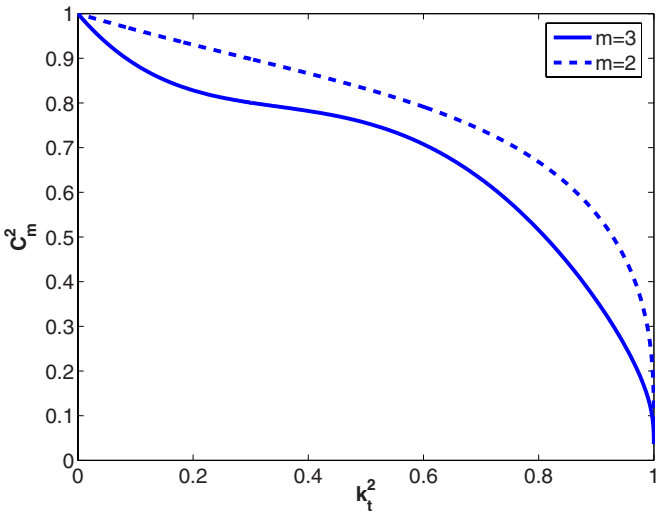

FIG. 5. (Color online) Pitch angle dependent factor after the bounce orbit average of the displacement eigenfunction, for the ideal kink mode from the cylindrical model.

toroidal plasma, with δW_f for a cylindrical equilibrium. Therefore, strictly speaking, our calculation for the RWM stability using Eq. (38) is consistent only at an infinite aspect ratio limit. It is possible to consider a more consistent, toroidal model with a truly pressure driven RWM.[45–47] Nevertheless, our approach here provides a simple, quantitative estimation of the drift kinetic effects on the growth rate of the mode. In a future work, we will perform full toroidal drift kinetic computations, without any approximations, using the updated MARS-F code.

The simple mode eigenfunction in a cylinder allows us to make an accurate calculation of the quantity $C_{l=0}=|\langle\xi_R\rangle|$ in Eq. (15). Indeed, for a given single Fourier harmonic m, we have $\xi_R=\xi_r\cos\theta-\xi_\theta\sin\theta=(m/F_0)r^{\mu-1}e^{i(m-\nu)\theta}$, hence

$$\langle\xi_R\rangle=\int_{-\theta_t}^{\theta_t}\xi_R\frac{d\theta}{|v_\parallel|}\left(\int_{-\theta_t}^{\theta_t}\frac{d\theta}{|v_\parallel|}\right)^{-1}$$

$$=\frac{m}{F_0}r^{\mu-1}\sum_{p=0}^{m-\nu}\binom{p}{m-\nu}(1-k_t^2)^{m-\nu-p}(2ik_t)^pK_p, \qquad (46)$$

where $k_t=\sqrt{(1-\lambda+\lambda\epsilon)/2\lambda\epsilon}$ (see the Appendix), and

$$K_p=\int_0^{\pi/2}(\sin\varphi)^p(\sqrt{1-k_t^2\sin^2\varphi})^{p-1}d\varphi/K(k_t),$$

$$p=0,1,2,\ldots,$$

where $K(k)$ is the complete elliptic integral of the first kind. We notice that $K_{p=0}=1, K_{p=1}=K^{-1}(k_t)$. Equation (46) is valid for $m-\nu\geq 0$. For $m-\nu<0$, we can use $\langle\xi_R\rangle_{m-\nu<0}=(\langle\xi_R\rangle_{|m-\nu|})^*$.

We write $C_{l=0}^2=(mr^{\mu-1}/F_0)^2C_m^2$ and consider two specific examples. If $m=2$ is the unstable RWM, we have $\nu=1, m-\nu=1$, and

$$C_{m=2}^2(\epsilon,\lambda)=C_{m=2}^2(k_t)=(1-k_t^2)^2+4k_t^2K^{-2}(k_t).$$

If $m=3$ is the unstable RWM, we have $\nu=1, m-\nu=2$, and

$$C_{m=3}^2(\epsilon,\lambda)=[(1-k_t^2)^2-4k_t^2K_2]^2+16(1-k_t^2)^2k_t^2K^{-2}(k_t).$$

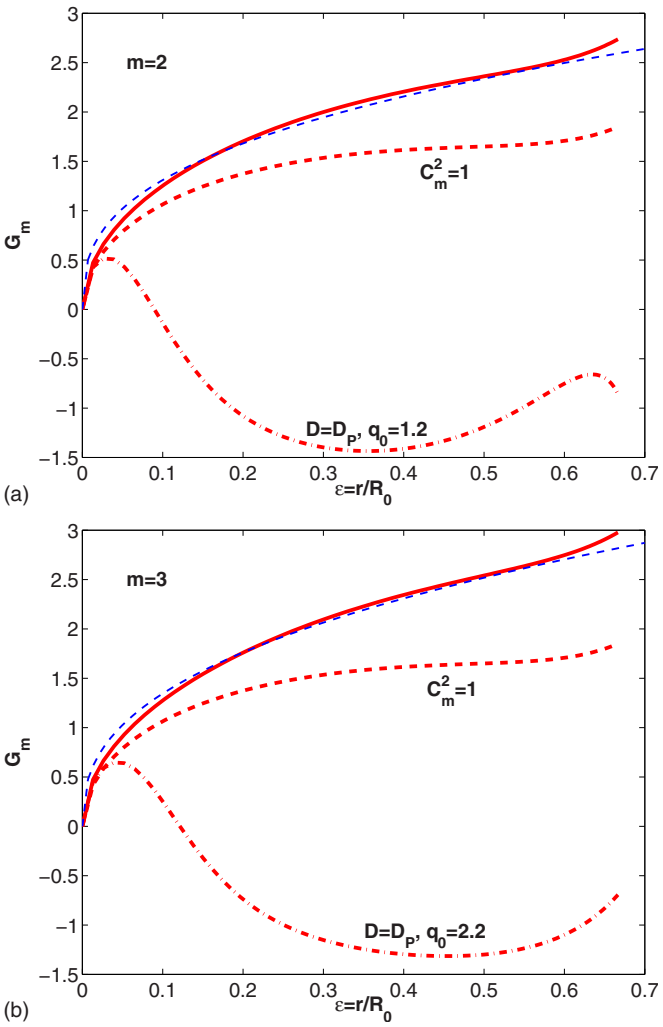

FIG. 6. (Color online) Radial profiles of the normalized integral G_m over velocity space, obtained after pitch angle integration under various assumptions, for the poloidal harmonic (a) $m=2$ and (b) $m=3$.

Figure 5 shows effectively the pitch angle dependence of the factor C_m^2 for $m=2$ and 3. For deeply trapped particles ($k_t=0$), $C_m^2=1$. For particles at the passing-trapping boundary ($k_t=1$), $C_m^2=0$. We have assumed $C_m^2(\lambda)\equiv 1$ in defining the pitch angle integrals G,S,Y in Eqs. (19), (22), and (34), respectively. We define a new factor G by including the pitch angle dependence of C_m^2,

$$G_m(\epsilon)\equiv\int_{1/(1+\epsilon)}^{1/(1-\epsilon)}d\lambda C_m^2\frac{(2-\lambda)^2}{FD}. \qquad (47)$$

Figures 6(a) and 6(b) show the real part of the $G_m(\epsilon)$ profiles under different assumptions, for $m=2$ and $m=3$, respectively. The curves with thick solid line include the full pitch angle dependence of C_m^2, whilst the thick dashed curves correspond to the normalized integral G over velocity space, as defined in Eq. (19) (different from Fig. 1, the magnetic shear here vanishes across the whole plasma). Neglecting the C_m^2 factor results in a reduction of the calculated drift kinetic energy by roughly 40%. This modification is quantitative rather than qualitative. The thick dashed-dotted curves in the

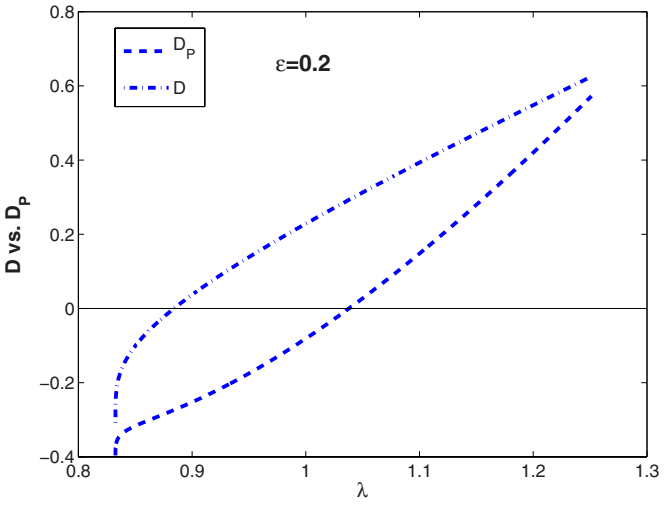

FIG. 7. (Color online) Example of modification of the pitch angle dependence of the normalized magnetic drift D, by the finite plasma pressure.

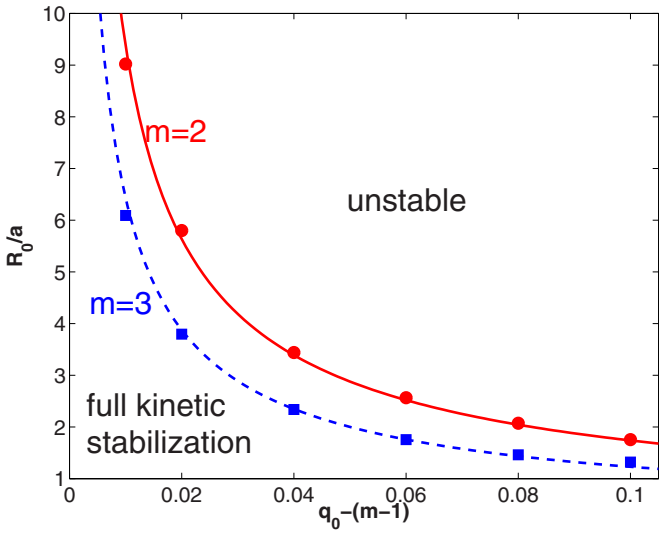

FIG. 8. (Color online) Critical curves in the R_0-q_0 plane for the $m=2$ and 3 unstable RWM, respectively. Below the curves, the mode is fully stabilized by the drift kinetic effect. The asymptotic case A is considered, with $C_p=0.5$ and without including the diamagnetic correction to the precession drifts. Note the smallness of the parameter space with a full kinetic stabilization.

figures show the effect of including the finite pressure correction to the precessional drift. This effect will be discussed following Fig. 7.

The thin dashed curves in Figs. 6(a) and 6(b) correspond to analytical approximations of the G_m factors as defined in Eq. (47), using the formula

$$G_m^{\mathrm{ana}}(\epsilon) = G_0 \epsilon^{\alpha_G}, \tag{48}$$

where $G_0=3$, $\alpha_G=0.36$ for $m=2$, and $G_0=3.3$, $\alpha_G=0.39$ for $m=3$. Substituting the analytical expression (48) into Eq. (18), and performing analytical integration over the minor radius, we obtain the real part of the perturbed drift kinetic energy for the asymptotic case A,

$$\mathrm{Re}[\delta W_k] = \frac{3\pi^2}{4}\frac{G_0}{\mu_0 q_0}\frac{m^2}{2\mu+1+\alpha_G}\frac{1}{(m+nq_0)^2}\frac{1}{R_0^{\alpha_G}}. \tag{49}$$

In the case of $C_p=0.5$, the imaginary part of δW_k vanishes due to the exact cancellation of the contributions between ions and electrons. Therefore, the stability of the kinetic RWM is determined by comparing Eq. (49) with Eq. (43), according to Eq. (38). The RWM is fully stabilized by the drift kinetic effects of trapped particles, for a plasma satisfying

$$R_0^{1.36} q_0 (m+nq_0)[1-(m+nq_0)] \lesssim 0.21, \quad (m=2),$$

$$R_0^{1.39} q_0 (m+nq_0)[1-(m+nq_0)] \lesssim 0.25, \quad (m=3).$$

Figure 8 plots these critical curves for the unstable $n=-1$ modes with $m=2$ and $m=3$, respectively, along with the calculated data points after numerical evaluation of Eq. (18). These curves of course become inadequate for small aspect ratios R_0. Nevertheless, they show that the plasma equilibrium parameter space, for which the kinetic RWM is stable, is very small and particular. A generic RWM will be unstable under the kinetic correction. The predicted stable region is even smaller if we do not consider the pitch angle dependence of $\langle \xi_R \rangle$.

The stable region in the R_0-q_0 plane practically vanishes if we take into account the finite pressure correction to the precessional drift frequency, Eq. (35), where $\alpha_P=4\epsilon$ for our plasma model. A comparison between D and D_P is shown in Fig. 7, for an example with $\epsilon=0.2$ and $q_0=2.2$. A distinctive feature is that these diamagnetic effects tend to shift the normalized magnetic drift D downwards, making it more negative. (This is also observed in toroidal calculations using MARS-F.) Because of the ϵ scaling ($\alpha_P=4\epsilon$), the effect is stronger towards the plasma edge. As a result, inclusion of D_P in the G_m evaluation, Eq. (47), switches its sign in a wide region close to the plasma edge, as shown by the thick dashed-dotted curves in Figs. 6(a) and 6(b).

Clearly this leads to a negative value for the δW_k according to Eq. (18). Hence, in this case we have a *destabilization* of the mode by the drift kinetic effects. This is shown in Figs. 9(a) and 9(b), for a static plasma with $q_0=2.2$, $C_p=0.5$ and an unstable $m=3$, $n=-1$ RWM. We have also assumed $\tau_w=10^4\tau_A$, $\nu_{\mathrm{eff}}=0$, $\omega_{ci}=10^2\omega_A$. The marginal ideal wall position for the ideal kink stability is $b_c/a=1.31$. The amplitude of both diamagnetic and precession drift frequencies is about $10^{-3}\omega_A$ (except $\omega_{*N}=0$ since we assume a flat density profile). Figure 9 shows the ratio of the kinetic modified growth rate (38) to the fluid one (45), versus the radius of the resistive wall, under three assumptions. The solid curves present a reduction of the RWM growth rate by the kinetic resonances, if we do not include the finite pressure modification to the precession drift frequency. The opposite case is presented by the dashed curves. In the former case, we obtain a partial stabilization of the mode. In the latter, the mode is destabilized by the kinetic effects due to the finite pressure modification to the drift frequency. If in addition to this, we include the fluid growth rate of the mode ($\omega=i\gamma_f$) in the resonance condition (14), we obtain the third curves (dashed-dotted), which show slight destabilization for least unstable RWM, and a weak stabilization for more unstable modes. Comparing cases (a) and (b), we notice that both

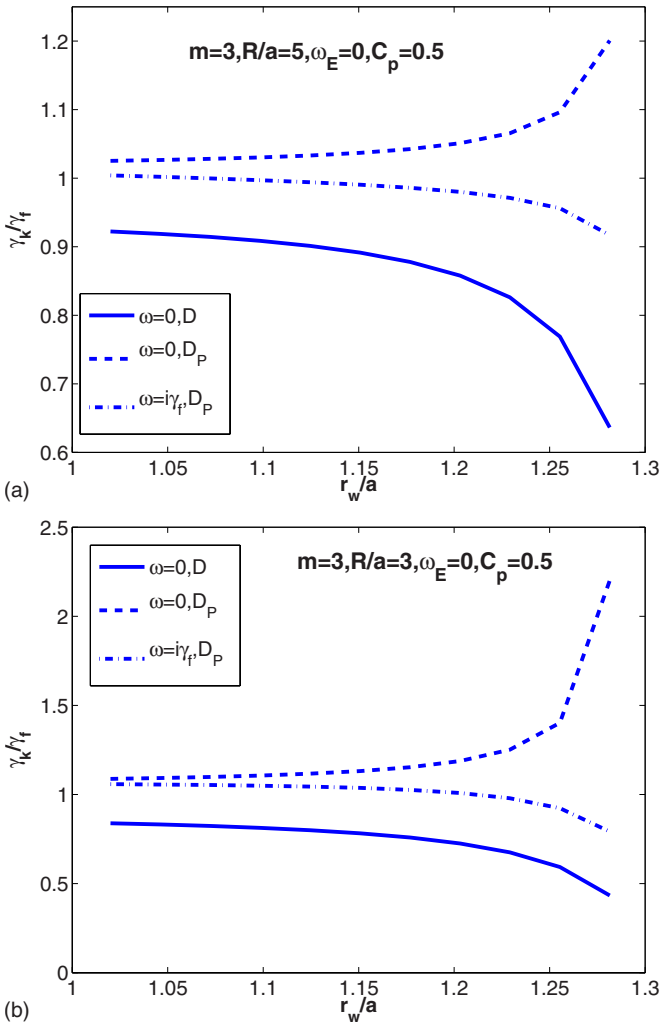

FIG. 9. (Color online) Stabilization/destabilization of the RWM by the drift kinetic effects under various assumptions. We assume $q_0=2.2$, $m=3$, $\omega_E=0$, and compare two equilibria with (a) $R_0=5$ and (b) $R_0=3$.

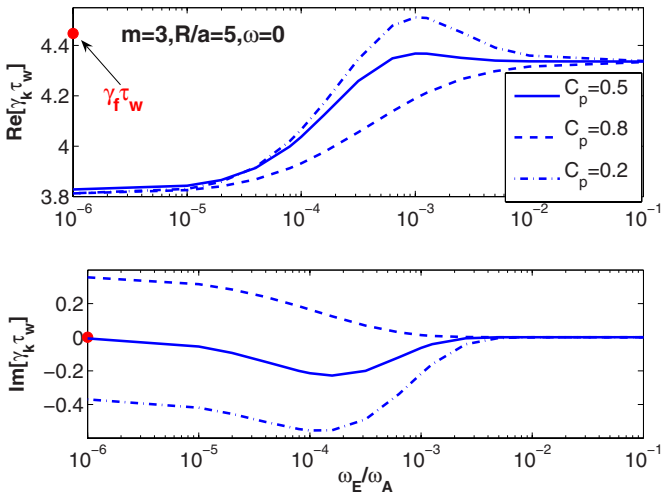

FIG. 10. (Color online) Effect of the plasma rotation on the drift kinetic modification of the RWM stability. We consider a case with $R_0=5$, $q_0=2.2$, $m=3$, $\omega=0$ and without inclusion of the diamagnetic correction to the precession drifts.

stabilizing and destabilizing effects are amplified by decreasing the aspect ratio R_0.

In Fig. 10, we perform a rotation scan of the growth rate for the kinetic RWM, assuming the same plasma parameters as in Fig. 9, except that we now consider only $\omega=0$, $b=r_w/a=1.2$, and without the finite pressure correction to the precession drifts. We choose three configurations for the ion/electron temperature ratio, corresponding to $C_p=0.5, 0.8, 0.2$. As a reference, we also indicate the fluid growth rate of the mode with no rotation. At the very slow rotation limit, we recover the asymptotic case A as described in Sec. III. Note that at this limit, with $C_p \neq 0.5$, the mode gains a finite frequency from the drift resonances, even in the absence of the plasma rotation. This is because of the finite net imaginary part of δW_k, which remains after cancellation between the ion and the electron contributions. At the limit of very fast plasma rotation, we recover the asymptotic case B (high frequency limit), which does not depend on the choice of the values for C_p. Note that generally there is no symmetry between the cases $C_p=0.8$ and $C_p=0.2$. This is not surprising, since the rotation shifts the precession drifts in different ways for ions and electrons, plus the fact that the normalized magnetic drift $D(\lambda)$ is not symmetric about its root.

V. SUMMARY AND DISCUSSIONS

We have performed an analytical, large aspect ratio, calculation of the perturbed kinetic energy, due to the RWM mode resonance with the magnetic precession drift motion of the trapped thermal ions and electrons. This has allowed us to isolate and illustrate the various physical effects that can occur in such a complex, multiparameter system. The analysis shows that both ion and electron resonances contribute to the kinetic energy perturbation. Four asymptotic cases are considered in detail.

At the limit of very slow plasma rotation (much lower than the precessional drifts), the drift kinetic energy is proportional to the plasma pressure gradient, associated with the particle diamagnetic drifts. The real parts of the contribution from ions and electrons add up, whilst the imaginary parts cancel between ions and electrons. The radial profile of the pitch angle integral G strongly depends on the magnetic shear.

At the opposite limit, when the plasma rotation is much higher than the precessional and diamagnetic drifts (but can still be lower than the ion bounce motion), we partially recover the Kruskal–Oberman high frequency kinetic term, which is proportional to the total plasma equilibrium pressure.

If the plasma rotation frequency is comparable to the diamagnetic frequencies, but much higher than the precession drift frequency, we obtain a first order FLR correction to the Kruskal–Oberman term. The correction term disappears if both ions and electrons have the same temperature, following an exact cancellation of their contributions. The next order correction term does not cancel between ions and elec-

trons, and is inversely proportional to the square of the rotation frequency. The radial shape of this contribution is not sensitive to the magnetic shear.

Finally, in the limit of a plasma with large electron collisionality, the drift kinetic energy, due to the electron resonance contribution, becomes inversely proportional to the effective collisionality coefficient, and proportional to the gradient of the product of the plasma equilibrium pressure and temperature. This is a pure damping term.

Considering a cylindrical plasma model allows us to scan the RWM growth rate modified by the kinetic terms, we found that a complete kinetic stabilization of the mode can occur only in a very narrow plasma equilibrium parameter space. Moreover, this stabilization is lost, or eventually switches to *destabilization* by including the finite pressure correction to the particle precession drifts, due to the fact that the pitch angle dependent factor D of the precession frequency becomes more negative, leading to a destabilizing kinetic energy contribution.

Analytical calculations show that this finite pressure correction to the precession drifts becomes more pronounced close to the plasma edge. If the RWM eigenfunction is modified by the kinetic effects in such a way that the displacement is pushed towards the edge, then it is easier to obtain a total negative drift kinetic energy contribution, which will cause destabilization of the mode. In this work, following the perturbative approach, we do not assume a kinetic modification of the fluid kink eigenfunction. A nonperturbative toroidal approach is in progress to include the drift kinetic terms self-consistently into the MHD equations.

ACKNOWLEDGMENTS

Y. Q. Liu thanks Dr. A. Thyagaraja and Dr. J. W. Connor from UKAEA Culham, and Professor J. Weiland from Chalmers University of Technology, for many fruitful discussions during this work. Suggestions made by Dr. T.C. Hender and I. T. Chapman to improve the manuscript are also gratefully acknowledged.

This work was partly funded jointly by the United Kingdom Engineering and Physical Sciences Research Council and by the European Communities under the contract of Association between EURATOM and UKAEA. The views and opinions expressed herein do not necessarily reflect those of the European Commission. This work was also supported by the U.S. Department of Energy under Contract No. DE-FG03-956ER54309.

APPENDIX: PARTICLE DRIFT FREQUENCIES

Here we define or briefly calculate various drift frequencies due to the particle bounce motion, magnetic precession, and the plasma diamagnetic effects. We assume a large aspect ratio plasma with a circular poloidal cross section, as described in Sec. II.

The diamagnetic drift frequencies due to the plasma density and temperature gradients are defined, respectively, as

$$\omega_{*N} = -\frac{\sigma_2 T}{2reB_0}\frac{d\ln N}{dr} = \sigma_2\frac{\rho_L}{r}\frac{v_{\rm th}}{R_0}\frac{1}{4\epsilon}\left(-\frac{r}{N}\frac{dN}{dr}\right),$$

$$\omega_{*T} = -\frac{\sigma_2 T}{2reB_0}\frac{d\ln T}{dr} = \sigma_2\frac{\rho_L}{r}\frac{v_{\rm th}}{R_0}\frac{1}{4\epsilon}\left(-\frac{r}{T}\frac{dT}{dr}\right),$$

where T is the plasma temperature for ions or electrons, each having the same amount of charge e, and the same density distribution $N(r)$. $v_{\rm th}\equiv\sqrt{2T/M}$ is the particle thermal velocity, $\rho_L\equiv v_{\rm th}/\omega_c$ the Larmor radius of the particle gyromotion, with $\omega_c\equiv eB_0/M$. The parameter $\sigma_2=1$ for ions and $\sigma_2=-1$ for electrons.

The bounce (transit) frequency of a passing particle is defined as

$$\omega_b^{\rm pass} = 2\pi\left(\oint\frac{dl}{v_\parallel}\right)^{-1},$$

where $dl\simeq R_0 q d\theta$, $\theta\in[-\pi,\pi]$. Using the lowest order approximation for the equilibrium field $B=B_0(1-\epsilon\cos\theta)$, a straightforward integration yields[10]

$$\omega_b^{\rm pass} = \frac{v_{\rm th}}{R_0}\frac{\sigma}{q}\left(\frac{\mathcal{E}_k}{T}\right)^{1/2}\frac{\sqrt{1-\lambda+\lambda\epsilon}}{\hat{K}(k_c)},$$

where $\hat{K}(k)=2/\pi\int_0^{\pi/2}d\varphi/\sqrt{1-k^2\sin^2\varphi}$ is the normalized complete elliptic integral of the first kind, $k_c=\sqrt{2\lambda\epsilon/(1-\lambda+\lambda\epsilon)}$ and $\sigma=\mathrm{sign}(v_\parallel)$.

The bounce frequency of a trapped particle is

$$\omega_b^{\rm trap} = 2\pi\left(\oint\frac{dl}{v_\parallel}\right)^{-1} \simeq \pi\left(\int_{-\theta_t}^{\theta_t} R_0 q\frac{d\theta}{|v_\parallel|}\right)^{-1},$$

where $\theta_t=\arccos[(\lambda-1)/\lambda\epsilon]$ is the turning point of the trapped particle. Assuming $k_t=\sin(\theta_t/2)=\sqrt{(1-\lambda+\lambda\epsilon)/2\lambda\epsilon}$ and $k_t t=\sin(\theta/2)$ (with t replacing the integration variable θ), we obtain

$$\omega_b^{\rm trap} = \frac{v_{\rm th}}{R_0}\frac{1}{2q}\left(\frac{\mathcal{E}_k}{T}\right)^{1/2}\frac{\sqrt{2\lambda\epsilon}}{\hat{K}(k_t)}.$$

Defining a normalized bounce frequency F

$$F = \begin{cases}\sqrt{2\lambda\epsilon}/\hat{K}(k_t), & \text{(trapped particles)}\\ \sqrt{1-\lambda+\lambda\epsilon}/\hat{K}(k_c), & \text{(passing particles)}\end{cases} \tag{A1}$$

we get a combined expression of ω_b for both passing and trapped particles

$$\omega_b = \frac{v_{\rm th}}{R_0}\frac{\sigma\sigma_1}{q}\left(\frac{\mathcal{E}_k}{T}\right)^{1/2}F,$$

where $\sigma_1=1$ for passing particles, and $\sigma_1=\sigma/2$ for trapped ones.

The derivation of the magnetic precession frequency ω_d is slightly involved, though well known for trapped particles.[38–40] We list here some key steps and a final expression, valid also for passing particles. We start with the definition

$$\omega_d = \langle \vec{v}_d \cdot \nabla \zeta \rangle, \tag{A2}$$

where $\zeta = q\theta - \phi$, and $\langle \cdot \rangle$ means average over the particle bounce orbit. The particle drift velocity $\vec{v}_d$,

$$\vec{v}_d = \frac{\sigma_2}{eB}\hat{b} \times (\mu \nabla B + M v_\parallel^2 \vec{\kappa}) \simeq \frac{\sigma_2}{eB_0 R_0}(\mu B + M v_\parallel^2)\hat{Z},$$

consists of the ∇B drift and the curvature drift. Since $\nabla \zeta = \hat{r}\theta q' + \hat{\theta} q/r - \nabla \phi$, and $\hat{Z} = \hat{r} \sin\theta + \hat{\theta} \cos\theta$, we obtain

$$\vec{v}_d \cdot \nabla \zeta = \frac{\sigma_2 q}{eB_0 R_0 r}(\mu B + M v_\parallel^2)(\cos\theta + s\theta \sin\theta), \tag{A3}$$

where $s = rq'/q$ is the magnetic shear.

We first perform the orbit averaging of the terms in Eq. (A3) associated with the ∇B drift. Following the procedure similar to the ω_b calculation, we derive

$$\langle B \cos\theta \rangle = B_0 \begin{cases} [2\hat{E}(k_t) - \hat{K}(k_t)]/\hat{K}(k_t), & \text{(trapped particles)} \\ [2\hat{E}(k_c) - (2 - k_c^2)\hat{K}(k_c)]/[k_c^2 \hat{K}(k_c)], & \text{(passing particles)} \end{cases} \tag{A4}$$

where $\hat{E}(k) = 2/\pi \int_0^{\pi/2} d\varphi \sqrt{1 - k^2 \sin^2\varphi}$ is the normalized complete elliptic integral of the second kind. The averaging over the $(\theta \sin\theta)$ term is performed in a similar way

$$\langle B\theta \sin\theta \rangle = B_0 \begin{cases} 4[\hat{E}(k_t) + (k_t^2 - 1)\hat{K}(k_t)]/\hat{K}(k_t), & \text{(trapped)} \\ 4[\hat{E}(k_c) - \sqrt{1 - k_c^2}]/[k_c^2 \hat{K}(k_c)]. & \text{(passing)} \end{cases} \tag{A5}$$

Next we consider the terms in Eq. (A3) associated with the curvature drift. For trapped particles, it can be easily shown that $\langle v_\parallel^2 \cos\theta \rangle$ and $\langle v_\parallel^2 \theta \sin\theta \rangle$ result in terms $O(\epsilon)$ smaller than those due to the ∇B drift. Therefore, we neglect the contribution from the curvature drift for trapped particles. However, for circulating particles, the curvature drift terms cannot be neglected due to a cancellation of the leading order terms in Eqs. (A4) and (A5). For these particles, we have

$$\langle M v_\parallel^2 \cos\theta \rangle = \frac{4\lambda \epsilon \mathcal{E}_k}{k_c^2 \hat{K}(k_c)} \left[\left(1 - \frac{2}{k_c^2}\right)\hat{E}(k_c) + \frac{2}{k_c^2}\hat{H}(k_c) \right], \tag{A6}$$

$$\langle M v_\parallel^2 \theta \sin\theta \rangle = \frac{16\lambda \epsilon s \mathcal{E}_k}{3k_c^4 \hat{K}(k_c)} [\hat{H}(k_c) - (1 - k_c^2)^{3/2}], \tag{A7}$$

where $\hat{H}(k) = 2/\pi \int_0^{\pi/2} d\varphi (1 - k^2 \sin^2\varphi)^{3/2}$.

Equations (A2)–(A7) lead to a final expression for the particle precession drift frequency

$$\omega_d = \frac{2\sigma_2 q \mathcal{E}_k}{eR_0 B_0 r} D = \sigma_2 \frac{\rho_L}{r} \frac{v_{\text{th}}}{R_0} q \left(\frac{\mathcal{E}_k}{T} \right) D$$

where we have introduced a factor D (normalized magnetic drift)

$$D = \begin{cases} \lambda[(2s+1)\hat{E}(k_t)/\hat{K}(k_t) + 2s(k_t^2 - 1) - 1/2], & \text{(trapped)} \\ [(1 - \lambda + \lambda\epsilon)/2\epsilon]\{[2s + 1 + 2\epsilon(1 - 2/k_c^2)]\hat{E}(k_c)/\hat{K}(k_c) + (4\epsilon/k_c^2)(1 + 2s/3)\hat{H}(k_c)/\hat{K}(k_c) + (k_c^2/2 - 1) - 2s\sqrt{1 - k_c^2}(1 - 4\epsilon/3 + 4\epsilon/3k_c^2)/\hat{K}(k_c)\}. & \text{(passing)} \end{cases} \tag{A8}$$

The precession frequency ω_d depends upon, among other variables, the particle energy $\mathcal{E}_k$, the pitch angle λ, and the magnetic shear s. At the trapped-passing boundary, $k_t = k_c = 1$, $\lambda = 1/(1+\epsilon)$, $D = -1/2(1+\epsilon)$ is the same for both trapped and passing particles, as expected. We also note that $D = 1/2(1-\epsilon)$ for trapped particles at $k_t = 0[\lambda = 1/(1-\epsilon)]$, and $D = s$ for passing particles at $k_c = 0(\lambda = 0)$. At the cylindrical limit $\epsilon \to 0$, $D = s(1 - \lambda/2)$ for passing particles.

[1] C. Kessel, J. Manickam, G. Rewoldt, and W. M. Tang, Phys. Rev. Lett. **72**, 1212 (1994).
[2] A. Bondeson, D. H. Liu, F. X. Söldner, M. Persson, Yu. F. Baranov, and G. T. A. Huysmans, Nucl. Fusion **39**, 1523 (1999).
[3] A. Polevoi, S. Yu. Medvedev, V. D. Pustovitov, V. S. Mukhovatov, M. Shimada, A. A. Ivanov, Yu. Yu. Poshekhonov, and M. S. Chu, *Fusion Energy 2002, Proceedings of the 19th International Conference*, Lyon, 2002 (IAEA, Vienna, 2002), CD-ROM file CT/P-08 and http://www.iaea.org/programmes/ripc/physics/fec2002/html/fec2002.htm.
[4] R. Aymar, P. Barabaschi, and Y. Shimomura, Plasma Phys. Controlled Fusion **44**, 519 (2002).
[5] C. G. Gimblett, Nucl. Fusion **26**, 617 (1986).
[6] A. Bondeson and D. J. Ward, Phys. Rev. Lett. **72**, 2709 (1994).
[7] R. Betti, Phys. Rev. Lett. **74**, 2949 (1995).
[8] J. Finn, Phys. Plasmas **2**, 198 (1995).
[9] M. S. Chu, J. M. Greene, T. H. Jensen, R. L. Miller, A. Bondeson, R. W. Johnson, and M. E. Mauel, Phys. Plasmas **2**, 2236 (1995).
[10] A. Bondeson and M. S. Chu, Phys. Plasmas **3**, 3013 (1996).
[11] R. Fitzpatrick and A. Y. Aydemir, Nucl. Fusion **36**, 11 (1996).
[12] C. G. Gimblett and R. J. Hastie, Phys. Plasmas **7**, 258 (2000).

[13]D. Gregoratto, A. Bondeson, M. S. Chu, and A. M. Garofalo, Plasma Phys. Controlled Fusion **43**, 1425 (2001).
[14]B. Hu and R. Betti, Phys. Rev. Lett. **93**, 105002 (2004).
[15]B. Hu, R. Betti, and J. Manickam, Phys. Plasmas **12**, 057301 (2005).
[16]Y. Q. Liu, A. Bondeson, M. S. Chu, J-Y. Favez, Y. Gribov, M. Gryaznevich, T. C. Hender, D. F. Howell, R. J. La Haye, and J. B. Lister, Nucl. Fusion **45**, 1131 (2005).
[17]L.-J. Zheng, M. Kotschenreuther, and M. S. Chu, Phys. Rev. Lett. **95**, 255003 (2005).
[18]E. J. Strait, T. S. Taylor, A. D. Turnbull, J. R. Ferron, L. L. Lao, B. Rice, O. Sauter, S. J. Thompson, and D. Wrblewski, Phys. Rev. Lett. **74**, 2483 (1995).
[19]A. M. Garofalo, A. D. Turnbull, M. E. Austin, J. Bialek, M. S. Chu, K. J. Comer, E. D. Fredrickson, R. J. Groebner, R. J. La Haye, L. L. Lao, E. A. Lazarus, G. A. Navratil, T. H. Osborne, B. W. Rice, S. A. Sabbagh, J. T. Scoville, E. J. Strait, and T. S. Taylor, Phys. Rev. Lett. **82**, 3811 (1999).
[20]A. M. Garofalo, T. H. Jensen, L. C. Johnson, R. J. La Haye, G. A. Navratil, M. Okabayashi, J. T. Scoville, E. J. Strait, D. R. Baker, J. Bialek, M. S. Chu, J. R. Ferron, J. Jayakumar, L. L. Lao, and M. A. Makowski, Phys. Plasmas **9**, 1997 (2002).
[21]R. J. La Haye, A. Bondeson, M. S. Chu, A. M. Garofalo, Y. Q. Liu, G. A. Navratil, M. Okabayashi, H. Reimerdes, and E. J. Strait, Nucl. Fusion **44**, 1197 (2004).
[22]T. C. Hender, M. Gryaznevich, Y. Q. Liu, M. Bigi, R. J. Buttery, A. Bondeson, C. G. Gimblett, D. F. Howell, S. D. Pinches, M. de Baar, P. de Vries, and JET EFDA Contributors, *Fusion Energy 2004, Proceedings of the 20th International Conference*, Vilamoura, 2004 (IAEA, Vienna, 2004), CD-ROM file EX/P2-22 and http://www-naweb.iaea.org/napc/physics/fec/fec2004/datasets/index.html.
[23]A. C. Sontag, S. A. Sabbagh, W. Zhu, J. M. Bialek, J. E. Menard, D. A. Gates, A. H. Glasser, R. E. Bell, B. P. LeBlanc, M. G. Bell, A. Bondeson, J. D. Callen, M. S. Chu, C. C. Hegna, and S. M. Kaye, Phys. Plasmas **12**, 056112 (2005).
[24]S. A. Sabbagh, A. C. Sontag, J. M. Bialek, D. A. Gates, A. H. Glasser, J. E. Menard, W. Zhu, M. G. Bell, R. E. Bell, A. Bondeson, C. E. Bush, J. D. Callen, M. S. Chu, C. C. Hegna, S. M. Kaye, L. L. Lao, B. P. LeBlanc, Y. Q. Liu, R. Maingi, D. Mueller, K. C. Shaing, D. Stutman, K. Tritz, and C. Zhang, Nucl. Fusion **46**, 635 (2006).
[25]H. Reimerdes, A. M. Garofalo, G. L. Jackson, M. Okabayashi, E. J. Strait, M. S. Chu, Y. In, R. J. La Haye, M. J. Lanctot, Y. Q. Liu, G. A. Navratil, W. M. Solomon, H. Takahashi, and R. J. Groebner, Phys. Rev. Lett. **98**, 055001 (2007).
[26]A. M. Garofalo, G. L. Jackson, R. J. La Haye, M. Okabayashi, H. Reimerdes, E. J. Strait, M. S. Chu, E. J. Doyle, J. R. Ferron, C. M. Greenfield, R. J. Groebner, Y. In, R. J. Jayakumar, M. J. Lanctot, G. Matsunaga, G. A. Navratil, C. C. Petty, J. T. Scoville, W. M. Solomon, H. Takahashi, M. Takechi, A. D. Turnbull, and The DIII-D Team, *Fusion Energy 2006, Proceedings of the 21st International Conference*, Chengdu, 2006 (IAEA, Vienna, 2006), CD-ROM file EX/7-1Ra and http://www-pub.iaea.org/MTCD/Meetings/fec2006pp.asp.
[27]E. J. Strait, A. M. Garofalo, G. L. Jackson, M. Okabayashi, H. Reimerdes, M. S. Chu, R. Fitzpatrick, R. J. Groebner, Y. In, R. J. LaHaye, M. J. Lanctot, Y. Q. Liu, G. A. Navratil, W. M. Solomon, H. Takahashi, and the DIII-D Team, Phys. Plasmas **14**, 056101 (2007).
[28]M. Takechi, G. Matsunaga, N. Aiba, T. Fujita, T. Ozeki, Y. Koide, Y. Sakamoto, G. Kurita, A. Isayama, Y. Kamada, and the JT-60 Team, Phys. Rev. Lett. **98**, 055002 (2007).
[29]J. L. Luxon, Nucl. Fusion **42**, 614 (2002).
[30]S. Takeji, S. Tokuda, T. Fujita, T. Suzuki, A. Isayama, S. Ide, Y. Ishii, Y. Kamada, Y. Koide, T. Matsumoto, T. Oikawa, T. Ozeki, Y. Sakamoto, and JT-60 Team, Nucl. Fusion **42**, 5 (2002).
[31]Y. Q. Liu, A. Bondeson, C. M. Fransson, B. Lennartson, and C. Breitholtz, Phys. Plasmas **7**, 3681 (2000).
[32]M. D. Kruskal and C. R. Oberman, Phys. Fluids **1**, 275 (1958).
[33]M. N. Rosenbluth and N. Rostoker, Phys. Fluids **2**, 23 (1959).
[34]R. J. Hastie, J. B. Taylor, and F. A. Haas, Ann. Phys. (N.Y.) **41**, 302 (1967).
[35]T. M. Antonsen and Y. C. Lee, Phys. Fluids **25**, 132 (1982).
[36]J. W. Van Dam, M. N. Rosenbluth, and Y. C. Lee, Phys. Fluids **25**, 1349 (1982).
[37]F. Porcelli, R. Stankiewicz, W. Kerner, and H. L. Berk, Phys. Plasmas **1**, 470 (1994).
[38]B. B. Kadomtsev and O. P. Pogutse, Sov. Phys. JETP **24**, 1172 (1967).
[39]Yanlin Wu, C. Z. Cheng, and R. B. White, Phys. Plasmas **1**, 3369 (1994).
[40]R. B. White, *The Theory of Toroidally Confined Plasmas*, 2nd ed. (Imperial College Press, London, 2001).
[41]J. W. Connor, R. J. Hastie, and T. J. Martin, Nucl. Fusion **23**, 1702 (1983).
[42]B. D. Fried and S. D. Conte, *The Plasma Dispersion Function* (Academic, New York, 1961).
[43]V. D. Shafranov, Sov. Phys. Tech. Phys. **15**, 175 (1970).
[44]J. A. Wesson, Nucl. Fusion **18**, 87 (1978).
[45]J. P. Freidberg and F. A. Haas, Phys. Fluids **16**, 1909 (1973).
[46]R. Betti, Phys. Plasmas **5**, 3615 (1998).
[47]S. J. Allfrey, A. Caloutsis, M. Coppins, C. G. Gimblett, R. J. Hastie, and T. J. Martin, in *Proceedings of the 25th EPS Conference on Plasma Physics and Controlled Fusion*, Praha, 1998, edited by P. Pavlo (European Physical Society, Praha, 1998), ECA Vol. 22C, pp. 2030–2033.